THE FORMATION OF CAPILLARY-GRAVITY WAVES BY A SUBMERGED CYLINDER IN A UNIFORM CURRENT

Roger Matsumoto Moreira, roger@vm.uff.br
LabCFD, PGEQ & PGMEC / School of Engineering / Fluminense Federal University
R. Passos da Pátria, 156, bl.D, sl.563A, Niterói, RJ, Brazil. CEP: 24210-240.

Abstract. *A submerged cylinder in a uniform stream flow is approximated by a horizontal doublet, following Lamb's classical method. Surface tension effects and a dipole are included in a fully nonlinear, unsteady, non-periodic, boundary-integral solver. Nonlinear effects are modelled by considering a flat free surface or a linear stationary solution as an initial condition for the fully nonlinear irrotational flow program. Long run computations show that these unsteady flows approach a steady solution for some parameters after waves have radiated away. In other cases the flow does not approach a steady solution. Interesting features at the free surface are found such as the appearance of "parasitic capillaries" near the crest of gravity waves and the formation of capillary-gravity waves upstream the cylinder.*

Keywords: *Free surface flow, water waves, boundary integral method.*

1. INTRODUCTION

The study of gravity waves formed at a free surface by the flow of a uniform stream interacting with a submerged cylinder has attracted the interest of researchers since the early 20th century. Kelvin was perhaps the first to suggest that problem in 1905, followed by Lamb who analysed it formally in the light of linear water wave theory in 1913 (for a more accessible version of this paper see Lamb 1932, § 247). Lamb's method consisted in replacing the cylinder by the equivalent doublet at its centre and then finding the fluid motion due to this doublet. Supposing a steady irrotational potential flow with a linearised free surface boundary condition, he found the appearance of a local disturbance immediately above the obstacle followed by a train of stationary, sinusoidal, gravity waves on the downstream side (see Fig. 1). This solution is applicable when the cylinder is of small radius compared with the depth of its axis; then the disturbance to the free stream due to the presence of the cylinder causes small amplitude waves that can be approximated by linear theory.

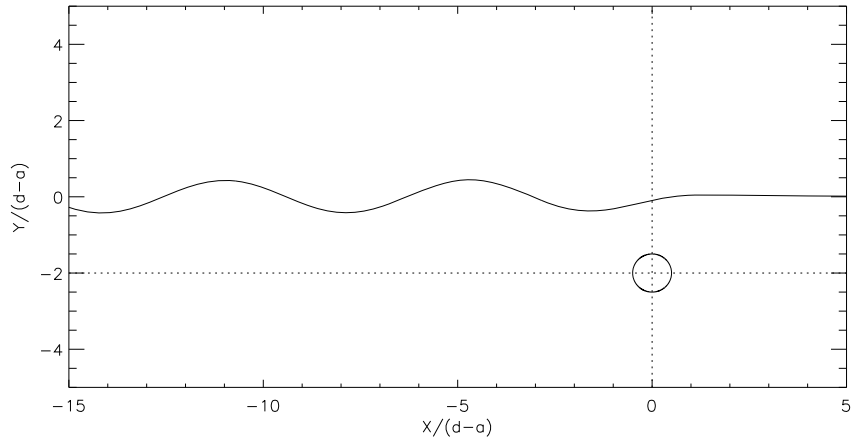

Figure 1. Stationary linear waves due to the presence of a cylinder of radius a and depth of submergence d on a uniform stream flow U, with surface tension effects neglected. $a/d = 1/4, U = -1$.

For large scale surface disturbances (of length greater than 10cm) this approximation is adequate; gravity is dominant and in the absence of wind the pressure exerted on the surface by the atmosphere can be considered constant. At a small scale, however, the surface pressure can be modified by surface tension. Capillary phenomena may arise when the surface possesses considerable curvature or when surface tension gradients appear on that surface. In both cases, the presence of these forces changes the nature of the free surface flow or induces motion originally absent (for full details see Moreira & Peregrine 2010). The present work reports an investigation of the effects of nonlinearity and surface tension at the free surface when a steady stream flow interacts with a submerged cylinder.

2. GOVERNING EQUATIONS

2.1 Unsteady nonlinear model

To model fully nonlinear effects at a free surface in a spatially non-periodic domain, the boundary-integral scheme described by Tanaka *et al.* (1987) is used as its starting point. An extension of the method which includes the modelling of unsteady free surface flows with surface tension implemented by Jervis (1996) is used to investigate the effects of surface tension. Following Lamb's classical method, the numerical scheme is adapted in order to include a horizontal doublet in a uniform stream flow defined by $\mathbf{U} = (U, 0)$. The fluid flow is assumed to be inviscid and incompressible with the single doublet located below the free surface at a depth of submergence d. It is also assumed that the flow is irrotational outside the singular core and away from the free surface. The irrotational velocity field $\mathbf{u}(x, y, t)$ is then given by the gradient of a velocity potential $\Phi(x, y, t)$ which satisfies Laplace's equation in the fluid domain, excluding the singular point. All the interior properties of the fluid are then determined by its properties at the boundaries alone. The entire motion can be modelled by considering a point discretisation of the surface. The solution method is based on solving an integral equation that arises from Cauchy's integral theorem for functions of a complex variable.

In order to apply Cauchy's integral theorem to the problem, the potential Φ must be known on all the boundaries. The kinematic and dynamic boundary conditions are applied at the free surface such that,

$$\frac{D\mathbf{r}}{Dt} = \nabla\Phi, \qquad \frac{D\Phi}{Dt} = \frac{1}{2}\,|\nabla\Phi|^2 - gy - \frac{p}{\rho}, \tag{1}$$

where $\mathbf{r} = (x, y, t)$, y is the elevation of the free surface above the undisturbed water level, g is the acceleration due to gravity and ρ is the fluid density. In the presence of surface tension, the pressure p exerted at the free surface is given by,

$$p = p_0 - \tau\frac{\partial^2\eta}{\partial x^2}\left[1 + \left(\frac{\partial\eta}{\partial x}\right)^2\right]^{-\frac{3}{2}}, \tag{2}$$

where τ is the surface tension coefficient. p_0 is the pressure on the exterior side of the surface and can be chosen to approximate the effects of wind or a localised pressure on the surface, though it is not used in the calculations. The last term in (2) refers to the contribution of surface tension effects to the pressure p which depends on the curvature of the free surface, defined by $y = \eta(x, t)$.

The fluid domain must be of finite extent in x for the purpose of computing a numerical solution. We approximate the desired "infinite" domain by assuming a finite extension in x that goes from, namely $-X_\infty$ to X_∞, which satisfies the following criterion,

$$|\nabla\Phi(\pm X_\infty, y, t) - \mathbf{U}| < \varepsilon, \tag{3}$$

valid for $-\infty < y \leq 0$ and $t > 0$. ε is a specified small "precision" parameter, while $\nabla\Phi(\pm X_\infty, y, t)$ is evaluated as explained in Dold (1992). For any time t, $\pm X_\infty$ are then determined iteratively by the numerical scheme; 10 equally spaced points are added to the far ends of the free surface until the criterion (3) is fully satisfied. Thus the distance between $-X_\infty$ to X_∞ is expected to increase with time due to the propagation of disturbances to the far field. It is also assumed that the water is deep, satisfying the condition $\nabla\Phi \to (U, 0)$ as $y \to -\infty$. To complete the model, an initial condition for the free surface is required such that $\eta(x, t) = \eta_0(x, 0)$ and $\Phi(x, \eta, t) = \Phi_0(x, \eta_0, 0)$. The numerical computations consider a flat free surface or the linear steady free surface profile derived in the following section as the initial condition for the fully nonlinear unsteady problem.

The introduction of a horizontal doublet in our model is done by decomposing our velocity potential Φ into a regular part ϕ_w (due to surface waves) and a singular part ϕ_s (due to the singularity) such that $\Phi = \phi_w + \phi_s$ (for more details see Moreira 2001). The velocity potential ϕ_s is then given by the real part of the complex potential for an irrotational flow due to an approximately circular cylinder held in a stream with uniform velocity U far from the cylinder (see Batchelor 1967, p.424). To apply Cauchy's integral theorem to the non-periodic free surface flow problem in deep water, the complex potential ω includes for convenience the reflection of the cylinder in the free surface,

$$\omega(z) = U\left(z - z_0 + \frac{a^2}{z - z_0} + \frac{a^2}{z - \overline{z}_0}\right), \tag{4}$$

where $z = x + iy$, $z_0 (= x_0 + iy_0)$ is the position of the centre of the cylinder, $\overline{z}_0$ its complex conjugate and a the radius of the cylinder.

2.2 Linear theory

From the theory of linear water waves and supposing that the surface waves propagate in deep water, surface tension effects are included in the dispersion relation such that the phase speed c satisfies,

$$c(k) = \left(\frac{g}{k} + \frac{\tau}{\rho}k\right)^{\frac{1}{2}}, \tag{5}$$

where k is the wavenumber. (For the purpose of calculations, we suppose $g = 980.6\text{cm/s}^2$, $\tau = 74.0\text{g/s}^2$ and $\rho = 1.0\text{g/cm}^3$.) The group velocity c_g of the surface waves are related to k by,

$$c_g(k) = \frac{c}{2}\left(\frac{\rho g + 3\tau k^2}{\rho g + \tau k^2}\right). \tag{6}$$

The linear dispersion relation represented by (5) has a minimum value at,

$$k = k_m = \left(\frac{\rho g}{\tau}\right)^{\frac{1}{2}}, \qquad c = c_m = \left(\frac{4g\tau}{\rho}\right)^{\frac{1}{4}}, \tag{7}$$

while the minimum group velocity is attained at $k = k_{g_m} = 0.40k_m$ and $c_g = c_{g_m} = 0.77c_m$. Here we define k_{g_m} and c_{g_m} as the wavenumber and speed at the minimum group velocity. For convenience expressions (5) and (6) are non-dimensionalised in terms of k_m and c_m reducing to,

$$\frac{c}{c_m} = \left[\frac{1}{2}\left(\frac{k}{k_m} + \frac{k_m}{k}\right)\right]^{\frac{1}{2}}, \qquad \frac{c_g}{c_m} = \frac{1}{2}\frac{c}{c_m}\left[\frac{(k_m/k)^2 + 3}{(k/k_m)^2 + 1}\right]. \tag{8}$$

The graphs of c and c_g against k in units of c_m and k_m are shown in figure 2.

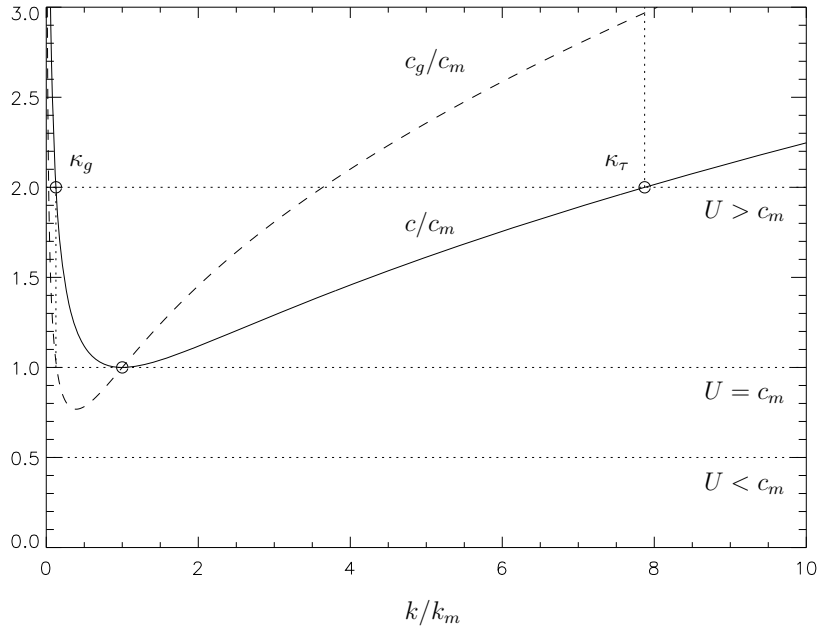

Figure 2. Phase speed and group velocity of capillary-gravity waves in deep water as a function of wavenumber, in units of c_m and k_m.

The waves produced by an obstacle on a uniform stream flow U may be viewed as the waves produced by the same obstacle moving with speed $-U$. In this frame of reference, supposing a two-dimensional problem, the only stationary waves that can keep up with the obstacle must satisfy the relation,

$$c(k) = U. \tag{9}$$

Therefore, if $U > c_m$, two solutions are possible, one coming from the gravity branch, namely k_g, and the other from the capillary branch, k_τ, such that $k_g < k_\tau$. These solutions can be associated to the group velocity through expression (8) such that,

$$c_g(k_g) < c(k_g), \qquad c_g(k_\tau) > c(k_\tau). \tag{10}$$

Since $c(k_g) = c(k_\tau) = U$, the capillary waves have a group velocity bigger than the stream velocity and therefore must appear ahead of the obstacle. The gravity waves must be downstream since their group velocity is slower than U.

When the stream velocity U is close to the minimum phase velocity c_m, the group velocity c_g is very close to U and the energy can move away from the pressure source only very slowly. As we approach c_m, a significant increase in wave steepness is associated to the linear solution and nonlinear effects start to become important. (Expressions for the linear wave amplitude and steepness are obtained and discussed in the next section.) The difference between c and c_g decreases until it completely vanishes as the two roots coalesce at c_m. At this point expressions for the linear wave amplitude and steepness become singular and the linear approximation breaks down. Based on the dispersion relation (5), if $U < c_m$, there are no solutions satisfying equation (9) and no wave can remain stationary on the stream. In this case there may exist local disturbances dying out away from the obstacle but no contribution to the asymptotic wave pattern. The disturbance level is then confined to a region about the pressure source represented by the obstacle and decays rapidly to zero with distance from it. For the critical case, viscosity becomes important and waves are damped very rapidly by it (for full details see Lamb (1932), §271).

For relatively deep water, two dimensionless parameters are defined for subsequent analysis – the Bond and the Froude numbers,

$$B = \frac{\tau}{\rho g (d-a)^2}, \qquad Fr = \frac{U}{\sqrt{g(d-a)}}. \tag{11}$$

3. FULLY NONLINEAR RESULTS

The numerical results here presented are obtained by applying the fully nonlinear, unsteady, boundary-integral scheme described in Dold (1992). When running the code the input data is set up such that $(d-a)$ corresponds to the characteristic length scale of the problem. The corresponding parameters that define the underlying flow i.e. the stream velocity U, the depth of submergence d and the radius of cylinder a, are also provided. The dipole is supposed to be at a fixed position in time. The initial conditions employed in the calculations are a flat free surface or the linear steady solutions derived in the previous section. Small disturbances associated to the impulsive motion of the problem may appear in the nonlinear results. In these cases long run computations are used aiming to obtain quasi-steady profiles. All the presented numerical simulations were computed on a Sun Ultra 2/200.

With the introduction of surface tension the linear dispersion relation has a minimum phase speed c_m which defines a region where waves do appear i.e. $U > c_m$. Two real roots then exist and, for $a/d \ll 1$, linear theory determines accurately the wave properties of the problem. However, if the ratio a/d increases, nonlinear effects may become important. If that is the case then the free surface profile is distorted and wave breaking may occur. For a constant d, as a/d assumes larger values, B also increases and thus surface tension effects may postpone wave breaking. Nonlinearity may also affect the free surface profile for values of $U < c_m$. Figure 3 shows the location of the nonlinear cases studied in this section with respect to the phase and group velocity of capillary-gravity waves. The fully nonlinear, unsteady, boundary-integral method is here employed taking into account the effects of surface tension. Special attention is directed to cases where $U < c_m$ i.e. $B > Fr^4/4$, with the ratio a/d assuming values sufficiently large for nonlinear effects to take place.

Figures 4a and 4b compares quasi-steady nonlinear results with linear steady solutions for cases (1) ($B = 0.0754$) and (2) ($B = 0.2218$) respectively, where $U > c_m$ (see figure 3). In these cases a flat free surface was used as the initial condition of the boundary value problem. Note that in both cases $a/d = 1/10$ and a vertical exaggeration of $10:1$ was used. As expected a good agreement was observed between the linear and nonlinear results, with "gravity-like" waves being formed downstream the cylinder and "capillary-like" waves ahead of it, which are visible only in case (2) where surface tension effects become more prominent ($B = 0.2218$). In both cases the nonlinear wave amplitudes give accurate linear solutions. When the ratio a/d is increased to $1/3$, keeping U/c_m and B with the same values, nonlinear effects take over and wave breaking occurs in both cases within very short times.

According to linear theory, if the value of U/c_m decreases, such that $U < c_m$, no real steady solution with waves exists for the phase speed, with only a local disturbance being predicted. However two roots exist for the group velocity if $c_m > U > c_{g_m}$, which may be associated to unsteady waves. Indeed the unsteady nonlinear computed cases (3) and (4) show that wave breaking occurs in this region. In fact case (3) has the calculations stopped at a shorter time ($t_{breaking} = 4.0$), supposing $B = 0.00302$, $a/d = 1/3$ and $U/c_m = 0.9052$ (see figure 5a for details). Figure 5b illustrates case (4), for which $B = 0.00582$, $a/d = 1/3$ and $U/c_m = 0.7681$. The time at which breaking occurs has now increased to 10.8. Since B is very small in both cases, surface tension effects are less prominent. The initial condition here used corresponds to the linear steady solution obtained in section 3. Due to the impulsive starting motion some capillary-gravity waves are visible propagating in the $-x$ direction. Waves are also formed ahead of the cylinder but these are "trapped" by the adverse stream flow U, with energy building up there until wave breaking occurs. Note that for case (4), U is very close to c_{g_m}.

For $U < c_{g_m}$ wave breaking was no longer observed in the unsteady nonlinear computations for constants $a/d\,(= 1/3)$ and $U\,(= -0.3)$. In fact, as B increases, U/c_m decreases and the capillary-gravity waves generated ahead of the cylinder

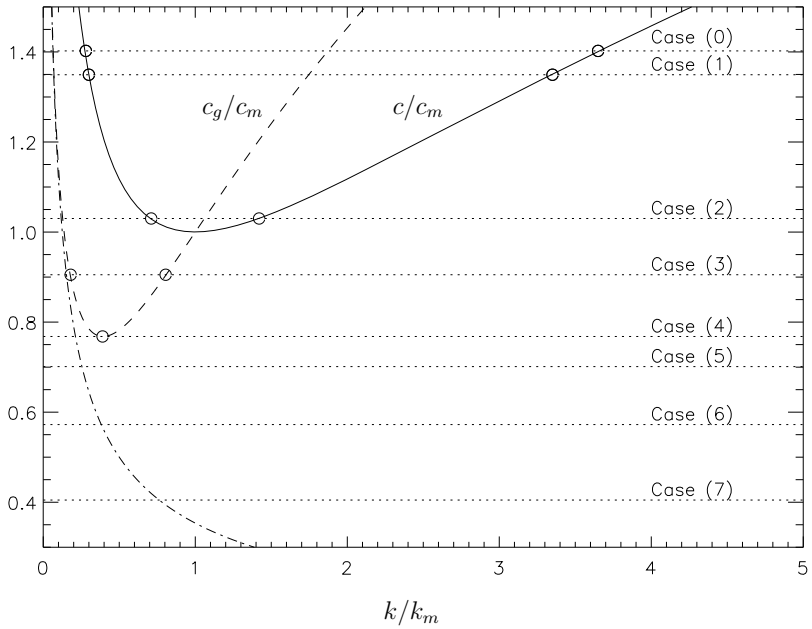

Figure 3. Location of the fully nonlinear results with respect to the phase and group velocity of capillary-gravity waves. The dashed-dotted line represents the group velocity of pure gravity waves. $k_m = B^{-1/2}$; $c_m = (4B)^{1/4}$. U, k, k_m, c, c_m and c_g are dimensionless quantities.

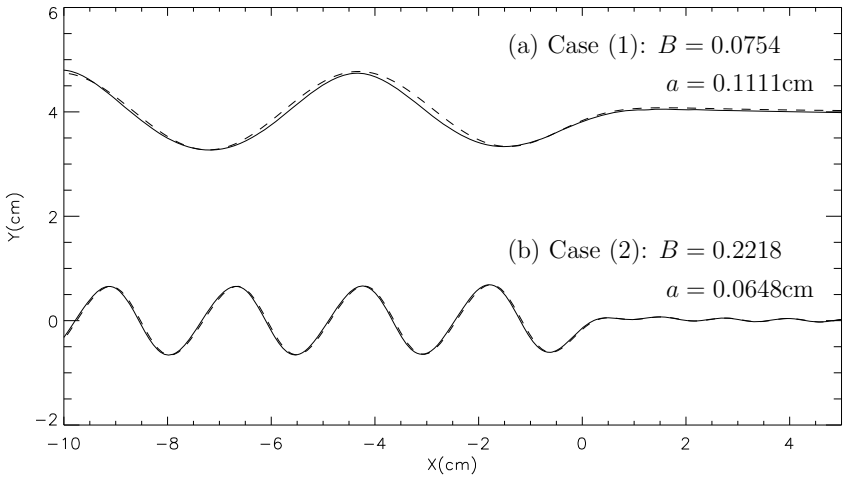

Figure 4. Comparison between quasi-steady nonlinear results (——) and linear stationary solutions (– – –). (a) $U/c_m = 1.3494$, $(d - a) = 1$cm; (b) $U/c_m = 1.0301$, $(d - a) = 0.583$cm. In the cases presented here $a/d = 1/10$, $U = -1$, $Fr = 0.75$ and $c_m = (4B)^{1/4}$. U and c_m are dimensionless quantities. Vertical exaggeration $10 : 1$.

are no longer "trapped" by the adverse current and now radiate upstream of the cylinder. This feature was observed in cases (5) to (7) for long computational runs (see figure 6), where $B = 0.00838$, 0.01885 and 0.0754, respectively. As B increases, surface tension effects become more important. Indeed capillary-gravity waves are formed as the underlying motion is switched on at time $t = 0$, generating unsteady waves that propagate in the $-x$ and $+x$ direction. The group velocity of the waves formed downstream of the cylinder is augmented by the following current and radiates away. On the other hand the group velocity of the capillary-gravity waves formed ahead of the cylinder is reduced by the adverse stream flow. As U/c_m keeps decreasing (since B increases), the stream velocity has less effect on the capillary-gravity waves generated until they are totally radiated away in both x directions, as shows figure 6.

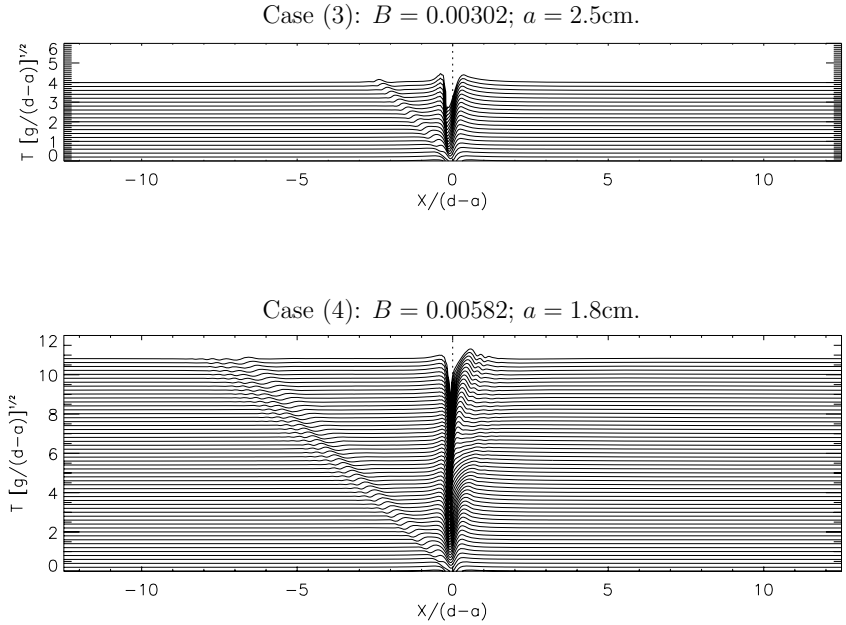

Figure 5. Fully nonlinear results for a uniform stream flow interacting with a submerged cylinder. (a) $U/c_m = 0.9052$, $(d-a) = 5.0$cm, $t_{breaking} = 4.0$; (b) $U/c_m = 0.7681$, $(d-a) = 3.6$cm, $t_{breaking} = 10.8$. In this case $a/d = 1/3$, $U = -0.3$, $Fr = 0.7$ and $c_m = (4B)^{1/4}$. U and c_m are dimensionless quantities. Vertical exaggeration $25:1$.

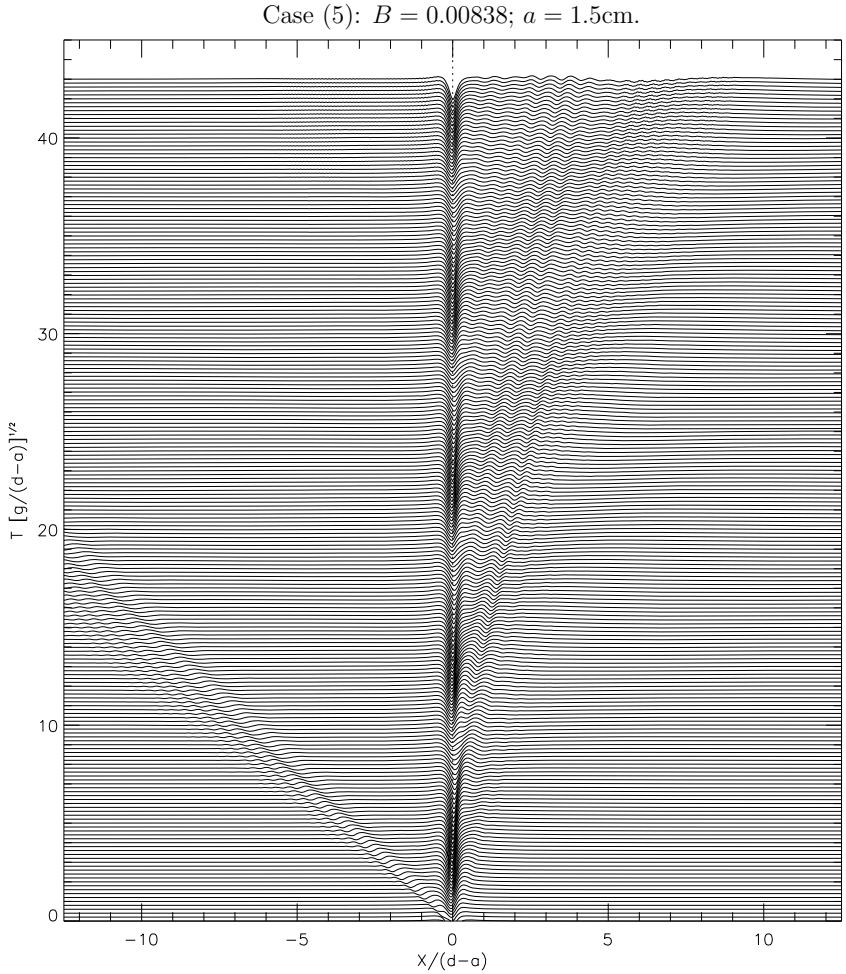

Figure 6. Fully nonlinear results for a uniform stream flow ($U = -0.3$) interacting with a submerged cylinder ($a/d = 1/3$, $Fr = 0.7$). $U/c_m = 0.7012$, $(d-a) = 3$cm. $c_m = (4B)^{1/4}$. U and c_m are dimensionless quantities. Vertical exaggeration $25:1$.

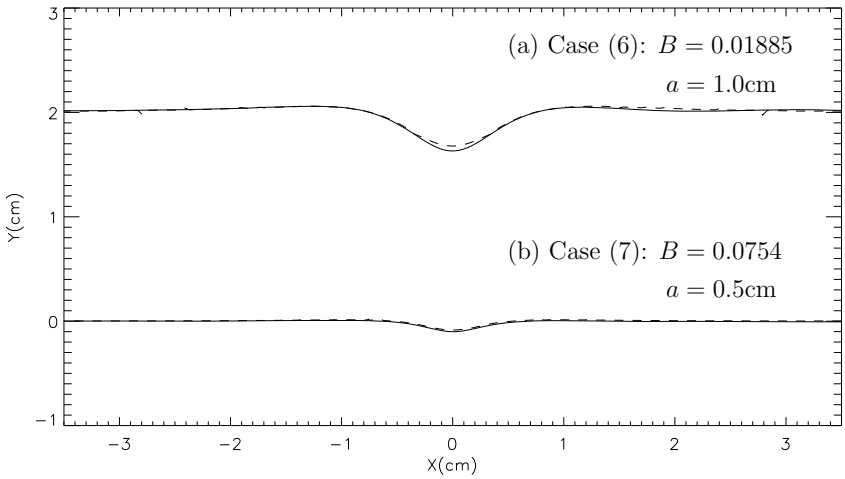

Figure 7. Comparison between nonlinear (——) and linear results (– – –). (a) $U/c_m = 0.5725$, $(d - a) = 2$cm; (b) $U/c_m = 0.4048$, $(d - a) = 1$cm. For all cases $a/d = 1/3$, $U = -0.3$, $Fr = 0.67$ and $c_m = (4B)^{1/4}$. U and c_m are dimensionless quantities. Disturbances are vertically exaggerated 10 times.

Comparisons between the linear and nonlinear wave profiles for cases (6) and (7) are presented in figures 7a and 7b. A vertical exaggeration of $10 : 1$ was employed at the free surface elevation in these cases. The linear steady solution behaves as a local disturbance, decaying rapidly to zero with distance from the cylinder, and thus it is used as the initial condition of the fully nonlinear problem. A good agreement was found between the linear and nonlinear results. Note also that the radius a is now not very different from the wavelength of the minimum group velocity $\lambda_{g_m} = 1.329$cm. As a increases, the free surface becomes more disturbed until wave breaking occurs (see figures 5 and 6).

Short capillary waves with wavelengths of several millimetres can often be seen near the crests of steep gravity waves with lengths between 5 and 25cm. This phenomenon was also observed in the unsteady nonlinear computations. Figure 8 shows the formation of "parasitic" capillary waves near the crest of gravity waves formed downstream the cylinder. In this case $B = 0.00378$, $a/d = 1/5$ and $U/c_m = 1.4023$. Due to the high curvature at the crest of the gravity wave, surface tension effects become locally important in this case, even though B assumes a small value. The capillary waves formed upstream the cylinder have a very small amplitude and cannot be noticed in figure 8. Note that the appearance of capillary waves downstream the cylinder is essentially a nonlinear phenomenon which is not predicted from group velocity concepts. The time at which breaking occurs is equal to 14.2.

4. CONCLUSIONS

The interaction between a free surface flow with surface tension and an approximately circular, horizontal cylinder is investigated. A fully nonlinear model which includes surface tension and a dipole in a stream flow was developed aiming to understand the behaviour of the free surface flow. A linear steady solution including surface tension effects was derived and employed as the initial condition of the nonlinear model in some of the computed cases.

For sufficiently small values of a/d, a good agreement between the quasi-steady nonlinear numerical results and the linear steady solutions is obtained for both pure gravity and capillary-gravity waves. However, as the ratio a/d increases, nonlinearity starts to play an important role. For pure gravity waves, the fully nonlinear results show that waves become "steeper", with sharper crests and shorter wavelengths, with wave breaking occurring when larger values of a/d are imposed.

With the introduction of surface tension, the numerical simulations have shown that wave breaking also occurs for sufficiently large values of a/d, but now this also depends on the Bond number B. As B increases, surface tension effects become more prominent; capillarity can then significantly reduce the steepness of the free surface disturbances when it precludes the formation of steady waves. For $U > c_{g_m}$ wave breaking was observed in all the computed cases when the inequality $a/d \ll 1$ was not satisfied. For $U < c_{g_m}$, an interesting feature was found: capillary-gravity waves are formed upstream the cylinder. According to linear theory, only a local disturbance which decays rapidly to zero with distance from the centre of the cylinder should happen in this case. However in an initial value problem waves can radiate away.

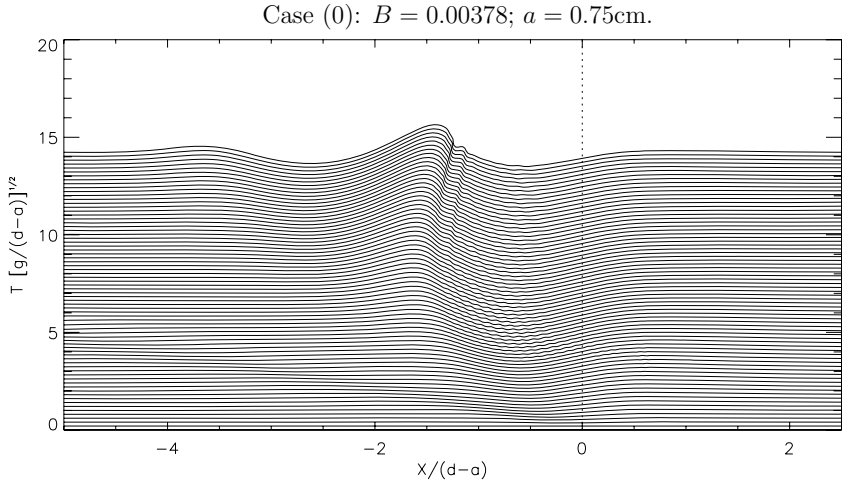

Figure 8. Fully nonlinear results for a uniform stream flow interacting with a submerged cylinder. $U/c_m = 1.4023$, $(d - a) = 3.0$cm. In this case $a/d = 1/5$, $U = -0.6$, $Fr = 0.44$ and $c_m = (4B)^{1/4}$. U and c_m are dimensionless quantities. $t_{breaking} = 14.2$. Vertical exaggeration $10 : 1$.

As U/c_m decreases, with values smaller than the minimum group velocity c_{g_m}, waves of all frequencies are radiated upstream and downstream. Then the nonlinear result approaches the linear steady solution of a local disturbance at the free surface.

5. ACKNOWLEDGEMENTS

R.M. Moreira acknowledges the financial support through CAPES, the brazilian agency for post-graduate education, and CNPq, the national research and development council (contract number 62.0018/2003-8-PADCT III / FAPERJ).

6. REFERENCES

Batchelor, G.K., 1967, "An Introduction to Fluid Dynamics", Cambridge University Press.

Dold, J.W., 1992, "An efficient surface-integral algorithm applied to unsteady gravity waves", J. Comput. Phys., v.103, pp.90–115.

Jervis, M.T., 1996, "Some Effects of Surface Tension on Water Waves and Water Waves at a Wall", PhD thesis, University of Bristol, U.K.

Lamb, H., 1932, "Hydrodynamics", 6th edition, Cambridge University Press.

Moreira, R.M., 2001, "Nonlinear interactions between water waves, free surface flows and singularities", PhD thesis, University of Bristol, U.K.

Moreira, R.M. and Peregrine, D.H., 2010, "Nonlinear interactions between a free surface flow with surface tension and a submerged cylinder", J. Fluid Mech., v.648, pp.485–507.

Tanaka, M., Dold, J.W., Lewy, M. and Peregrine, D.H., 1987, "Instability and breaking of a solitary wave", J. Fluid Mech., v.185, pp.235–248.

7. Responsibility notice

The author is the only responsible for the printed material included in this paper.